Proceedings World Geothermal Congress 2010
Bali, Indonesia, 25-29 April 2010

Acid Well Utilisation Study: Well MG-9D, Philippines

K.A. Lichti[1], S.P. White[2], M. Ko[1], R.R. Villa, Jr.[3], F.L. Siega[3], M.M.M. Olivar[3], N.D. Salonga[3], M.S. Onega[3], S.E. Garcia[3], B.C. Buning[3], N. Sanada[4]

[1]Quest Reliability Ltd., Gracefield Research Centre, Lower Hutt, New Zealand
[2]Industrial Research Ltd., Gracefield Research Centre, Lower Hutt, New Zealand (Author Deceased)
[3]PNOC Energy Development Corporation, Meritt Road, Ft. Bonifacio, 1201 Makati City, Philippines
[4]Tohoko National Industrial Research Institute AIST, MITI, Sendai, Japan

k.lichti@questreliability.com[1]

Keywords: carbon steel, acid, geothermal, well, corrosion, control, pH, scaling, corrosion product

ABSTRACT

Acid wells have been found in many shallow geothermal reserves, but production from acidic geothermal wells is not yet common. The ability to safely and cost effectively produce such wells depends on the well chemistry and the selected corrosion control method.

An acid well, MG-9D was produced for a short period of testing with and without NaOH injection just below the wellhead to demonstrate the mechanism of corrosion control using corrosion coupons and on-line monitoring probes.

Carbon steels exposed to the unaltered acid well process steam corroded at rapid unacceptable rates whereas pH adjusted fluid had immediate reduction in corrosion rate. This paper will demonstrate the mechanisms of corrosion control - a mix of corrosion product formation and scaling.

1. INTRODUCTION

Acid wells have been encountered in both deep and shallow geothermal reserves. (Sanada et al, 2000) Production from acidic geothermal wells where the acidity is derived from acid sulfate (chloride) waters has been successfully achieved by controlled injection of NaOH for downhole pH adjustment. (Sanchez et al, 2000, Moya et al, 2005) The ability to safely and cost effectively produce such wells depends on the well chemistry and selected corrosion control method.

Mahanagdong is one of the fields that has encountered acidic well fluids. It is located in the island of Leyte, Philippines (Figure 1). This sector is part of the Greater Tongonan Geothermal Field developed and operated by PNOC Energy Development Corporation (PNOC-EDC). Mahanagdong has a total installed plant capacity of 198MW composed of three units of 60MW condensing turbine modules and three units of 6MW high pressure non-condensing turbine modules (Villa et al, 1999).

A total of four wells were drilled in the area targeted by MG-9D. These wells produced highly corrosive fluids with a pH range of 2.9-3.4. Earlier corrosion testing at MG-21D showed that the acid fluids can corrode carbon steel at a maximum rate of 0.23mm/day (Parrilla et al., 1996). This corrosion rate is detrimental to the field operation since the fluids will damage the carbon steel well casing and surface pipelines also made of carbon steel.

Calciting of production wells at Mahanagdong has caused concern over decreasing steam supply for the sector. A few long term solutions have been proposed, one of which included the utilization of acidic wells for production purposes. However, this would only be possible provided that the acidity can be controlled.

pH adjustment of acidic thermal surface waters has been tested as a means of corrosion control Lichti and White, 1998, Lichti, White and Sanada., 1998) for deep and acidic geothermal wells. This report summarizes the results of downhole testing of the possible benefits of pH adjustment for corrosion control in the acidic fluids of well MG-9D. Well MG-9D was chosen as an experimental well for this study for a number of logistical reasons including its proximity to other wells that could be used for well stimulation.

2. TEST ENVIRONMENT CHEMISTRY

A study conducted in 1997 (Salonga et al., 1997) in Mahanagdong acidic wells showed that the well discharged an acid Cl-SO_4 type of fluid. The acid fluid discharge of well MG-9D was not an active magmatic contribution but rather caused by incomplete equilibriation between the rocks and the fluids.

The major acid species (HSO_4^-) is a weak buffer at higher temperature and it cannot initiate rock dissolution process which would effectively scrub-off the free H^+. However, as the temperature drops, the fluid dissociates to SO_4^{-2} and liberates the H^+ which makes the fluid highly acidic.

MG-9D was drilled from August 19 to December 14, 1993. When it was discharged in April 1994, it yielded a very low pH fluid suggesting an occurrence of strong acid contributions. The suspected acid zones were plugged at 1550-1650 mMD and 1750-1800 mMD. However, the post plugging discharge yielded similar acid fluids. Discharges in 1999 again yielded a similar acid fluid. The discharge fluid was characterised as acid chloride-sulfate with a pH range of 2.9 to 3.4 at laboratory conditions. The chloride and silica ranged from 5000-6000 mg/kg and 700-900 mg/kg, respectively, which were comparable to the concentration of the upflow fluids in the sector (Villa et al, 2000).

The water phase chemistry (Table 1) also showed a significantly higher value of $SO^{4=}$, Fe and Mg typical of acid wells in the area. The high Fe in the discharge could have come from the corrosion of the carbon steel casing itself. Table 2 summarizes the gas concentrations at different periods. The H_2S level of the well MG-9D was the highest among the Mahanagdong wells.

Table 1: MG-9D water chemistry

DATE	WHP (MPaa)	H (kJ/kg)	SP (MPaa)	pH (25°C)	Na	K	Ca	Mg	Fe	Cl	SO_4	B	NH_3	SiO_2	H_2S
					(in mg/kg)										
Previous Discharge Data															
26-Apr-94	1.874	1287	0.480	3.11	3117	950	82	25.00	282.00	6175	508	21	15.60	910	0.95
18-Feb-95	2.693	1554	0.480	3.24	3450	1200	90	16.75	53.00	6415	101	23	19.40	1003	2.22
1999 Discharge Data															
04-Jul-99	0.838	1122	0.793	3.43	3039	617	72	10.80	96.65	5263	300	54	11.85	571	5.80
24-Aug-99	0.838	1122	0.903	3.16	2782	538	96	10.70	65.39	5046	310	56	9.66	575	3.30
26-Aug-99	0.838	1122	0.903	2.87	3362	668	94	12.05	69.78	6088	380	64	12.08	691	1.40
07-Sep-99	0.993	1152	0.943	4.05	2836	564	92	10.40	69.24	4947	315	49	12.99	569	3.80

Table 2: MG-9D gas chemistry

DATE	WHP (MPaa)	Enth (kJ/kg)	SP (MPaa)	CO_2	H_2S	NH_3	He	H_2	Ar	N_2	CH_4
				(mmole/100 moles steam)							
Previous Discharge Date											
26-Apr-94	1.874	1287	0.480	400	24.26	0.05	0.000	0.082	0.051	12.667	0.648
18-Feb-95	2.693	1554	0.480	628	36.34	0.03	0.000	0.646	0.000	4.213	1.023
1999 Discharge data											
04-Jul-99	0.838	1122	0.793	120	16.00	0.01	0.047	1.313	0.318	1.282	0.129
24-Aug-99	0.838	1122	0.903	165	9.60	0.00	0.001	2.682	0.038	2.306	0.434
26-Aug-99	0.838	1122	0.903	195	10.70	0.00	0.000	4.381	0.026	1.623	0.387
07-Sep-99	0.993	1152	0.943	184	18.40	0.20	0.002	10.468	0.000	9.559	1.657

Table 3: Well MG-9D Wellbore geometry for Well MG-9D (Salonga, 1998). Reservoir temperature was 298°C.

Well Depth	1940.4 mMD	
	1686.4 mVD	
Casing Size and Depth	20”	109mMD CHF
	13 3/8”	689.8 mMD 663.9 mVD
	9 5/8”	1433.5 mMD 1279.2 mVD
	7 5/8”	1934.4 mMD 1678.2 mVD

Note: MD: measured depth
VD: vertical depth

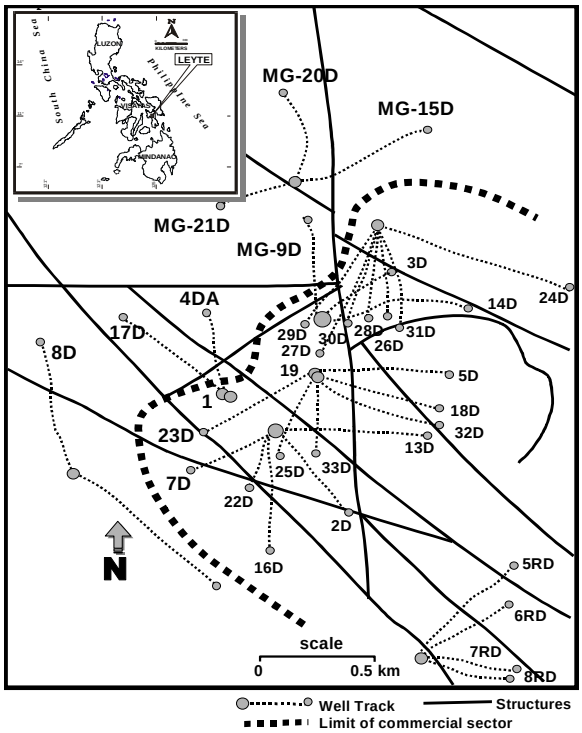

Figure 1: Map of Mahanagdong geothermal field showing Well MG-9D.

The 1994 and 1995 discharges had higher ionic concentrations except for $SO_4^{=}$ and B. The variation in chemistry within these periods suggests that the initial injected drilling fluids had not been cleared. This was manifested by the higher Cl, SiO_2, and SO_4 which indicated the presence of drilling mud. The well was also used periodically for brine and condensate disposal. The 1999 discharge analyses had a lower concentration of these components suggesting that the well had been cleared of the above-mentioned impurities.

A model of the wellbore chemistry (Lichti and White, 1998, Lichti, White and Sanada, 1998) was developed for the length of the wellbore using the available data of well chemistry (Table 1 and 2), the wellbore geometry (Table 3) and assuming a flow rate of 120 kg/s from the well. The results are shown in Figure 2. These authors argued that the well fluid pH corrosivity at pH 5 to pH 4.5 would give a low and acceptable corrosion rate. Injection of NaOH to 600 m to raise the pH above 4.5 from that level was proposed as a means of achieving corrosion free wellbore fluid production. The aim of the corrosion testing was therefore to inject NaOH to raise the pH to 4.5 and prove that the corrosion rates would be low and acceptable.

3. EXPERIMENTAL PROCEDURES

The corrosion mitigation testing of Well MG-9D was completed in three stages. The first stage was conducted on July 4, 1999 by discharging the well to clear it from all debris and condensate fluids. The baseline chemistry of the fluid was also established.

The second stage commenced on August 24, 1999. It was aimed to establish the on-line corrosion rates using weight loss metal coupons immersed in the discharging line (Figure 3). Ultrasonic testing (UT) of the discharge pipelines and on-line corrosion rate monitoring devices (LPR electrodes and Corrosometer probes) were also used. The first corrosion test (Test 1) was conducted without injecting any chemicals and was intended to provide the baseline corrosion rate data for the acid well fluids. Stage 3 commenced in August 25, 1999, when the testing resumed by injecting a NaOH solution into the well using a ¼-inch diameter Incoloy 825 tubing set at 205 mMD (Test 2). The injection set up is shown in Figure 4. New metal coupons were used, while UT and other on line corrosion rate

measurements were also conducted. As the testing progressed, it was observed that the pH decreased from 3.9 to 3.0 and remained at this value despite the diluted NaOH being injected at the maximum allowable concentration for the materials being used and at the maximum rate of the available pumping equipment.

Based on the observations and analysis made, it was concluded that the volume of chemicals injected was insufficient to elevate the pH of the fluid (Figure 5) to the target of pH > 4.5. This problem was mainly attributed to the limited injectate volume that could be handled by the small diameter tubing.

On September 7, 1999, the third stage of NaOH testing (Test 3) continued when a one-inch sucker rod was used and set at a depth of 20 mMD. At the maximum pump stroke, the dosing rate of NaOH solution was sufficient to alter the pH to 5.5 when the pH was around 4.1. The initial pH increase when NaOH was injected (Figure 6) could not be maintained at the target pH of 4.5 as the produced well fluids become more acid. At the completion of the NaOH test (Test 3), other corrosion inhibitors were also tested including CorrFree and Nalco 1800 and with these fluids the well acidity stabilised at 2.9, then 2.8 (Figure 6).

The corrosion coupons remained in the pipeline for these additional tests and so their results are not further considered. The on-line monitors were removed to provide a means of fully evaluating the effects of NaOH injection.

Mass loss coupons present a major difficulty with respect to the conducting of timed exposure in field work; that is in achieving the desired condition throughout the test programme. In this regard, on-line monitors can give improved opportunity to measure short term corrosion rates. Analysis following exposure for corrosion product and scale properties is essential to qualify the result of both mass loss coupons and on-line monitors.

3.1 On-line Corrosion Monitoring Test Matrix

On-line Electrical Resistance (ER) Corrosometer probes, Linear Polarisation Resistance (LPR) probes and weight loss coupons were used as shown in Figure 7. A Silver/Silver Sulfide reference electrode was used to measure corrosion potentials of the LPR electrodes. The electrodes were made using the method described in Crowe and Tromans, 1986. The monitors used for evaluating the corrosion properties are detailed in Table 4.

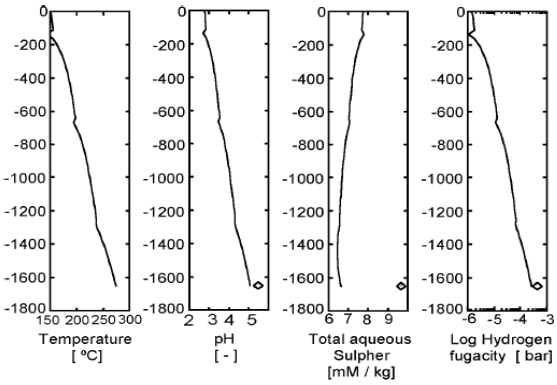

Figure 2: Wellbore chemistry modelling (Lichti, White and Sanada, 1998). The diamonds represent values for liquid water at 300°C.

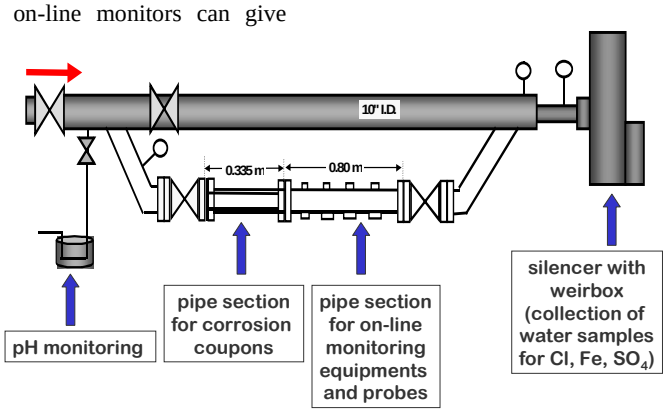

Figure 3: MG-9D discharge line monitoring set-up.

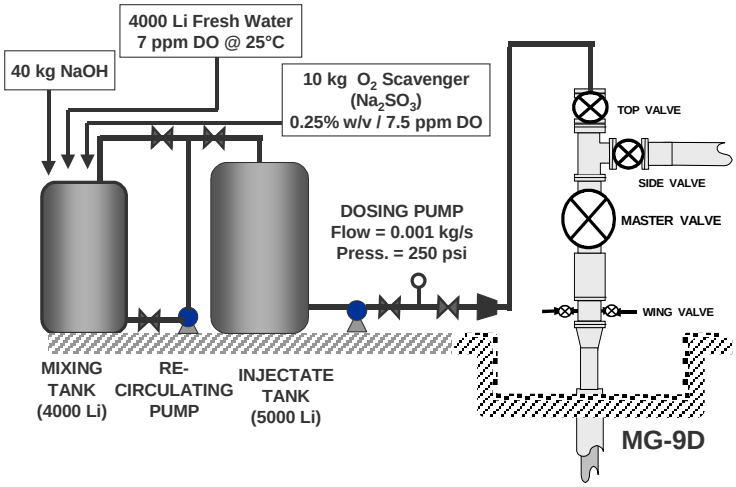

Figure 4: Process flow diagram of injection set-up.

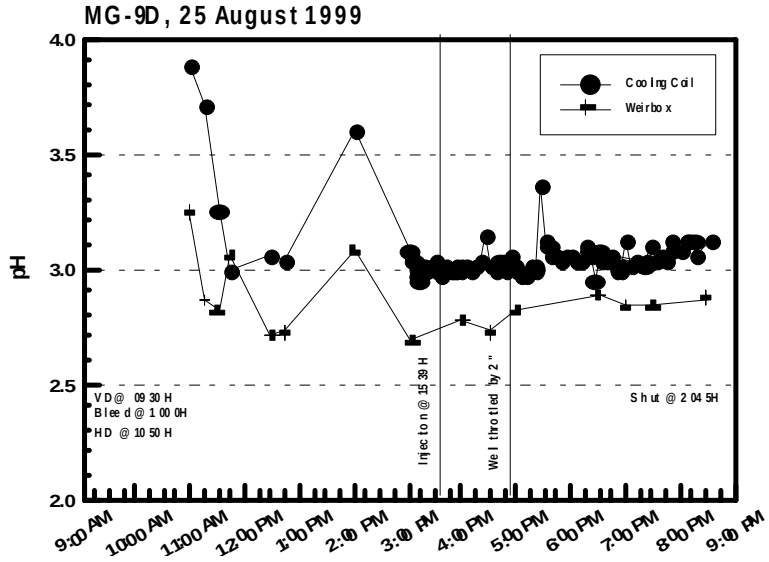

Figure 5: The pH trends of MG-9D during NaOH injection using Incoloy 825 tubing (Test 2).

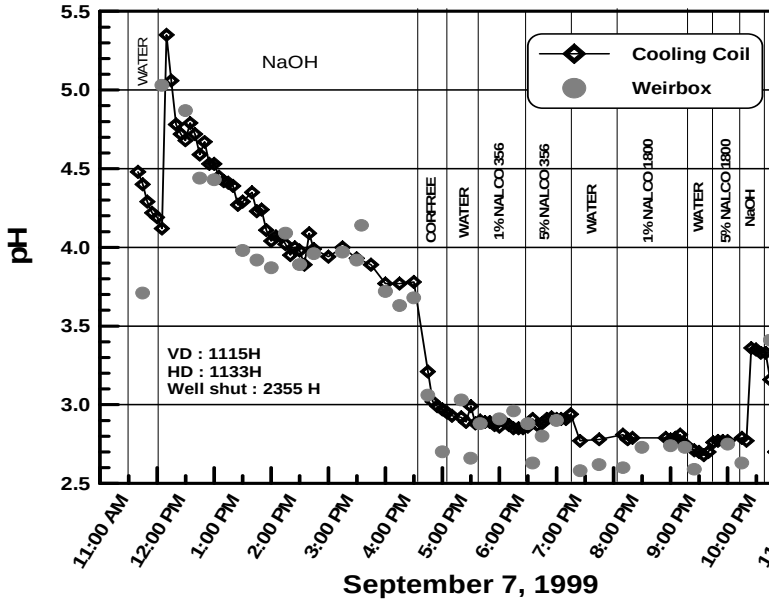

Figure 6: MG-9D pH Trend during NaOH injection using 1-inch sucker rod (Test 3 was completed at 4pm).

4. RESULTS

Results obtained from the exposed coupons (Test 1) and from the UT wall thickness measurement of the casings and piping has been previously published (Villa et al, 2000). Results obtained from Linear Polarisation Resistance (LPR) probes and Electrical Resistance (ER) probes have now been evaluated to further explore the mechanisms of corrosion control.

4.1 Corrosion Rates

The corrosion rates measured and calculated using the weight loss method of the corrosion test coupons in the pipeline (Villa et al, 2000) was supplemented by the UT testing, weight loss measurement on the LPR electrodes as well as on-line results from the LPR and Electrical Resistance monitor.

Coupons and Mass Loss on LPR Electrodes

For the corrosion coupons and electrodes, the material loss was defined as the mean thickness of the material lost by corrosion during an exposure period based on change in mass (Braithwaite and Lichti, 1980):

$$ML = \left(\frac{\delta}{\rho A} \right) \times 10^3 \qquad (1)$$

where ML = Material loss (μm); δ = Weight loss (mg), ρ = Material density (mg/mm^3) and A = Exposed area of material (mm^2).

Using the weight loss method, the corrosion rate may be calculated as follow:

$$CR = \frac{(ML \times const)}{t} \quad , \qquad (2)$$

where CR = Corrosion rate (μm/yr), ML = Material loss (μm), $const$ = 31.557×10^6 (s/mean solar yr) and t = Exposure period (s).

Table 4: Details of corrosion testing including the weight loss coupons in the pipeline and on-line corrosion monitoring.

	Test 1	Test 2	Test 3
Corrosometer Probe			
Steam (static)	Carbon Steel	Carbon Steel	Carbon Steel
Steam (in the flow)	Stainless Steel 316	Carbon Steel	Carbon Steel
Brines liquid	Carbon Steel	Carbon Steel	Carbon Steel
LPR Probe/Weight Loss Electrode			
Bottom	Carbon Steel	Carbon Steel	Carbon Steel
F1 Cross	Carbon Steel	Carbon Steel	Carbon Steel
F2 Cross	Incoloy 825	Incoloy 825	Incoloy 825
G1 Well	Sandvik 2205 Sandvik 2507	Sandvik 2205 Sandvik 2507	Sandvik 2205 Sandvik 2507
Weight Loss Pipeline Coupons			
PNOC-EDC	Carbon Steel	Carbon Steel	
TNIRI	Carbon Steel 22Cr5Ni (2205)	Carbon Steel 22Cr5Ni (2205)	
Reference Electrode	Ag/AgS	Ag/AgS	Ag/AgS

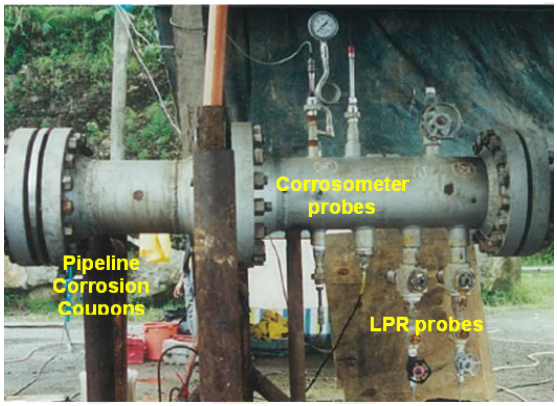

Figure 7: Corrosion test rig showing location of the pipeline corrosion coupons and other on-line corrosion monitoring.

The weight loss results for the coupons for acid fluid in the pipeline (Test 1) are summarised in Table 5. The corrosion rates were calculated by observing the material loss on the sample (after electrochemical cleaning to remove the retained corrosion products) over the exposure period and extrapolating the result to one year.

The mass loss results from these short term tests when extrapolated to one year are prone to error, i.e. the single exposure test time does not take into account small changes of corrosion mechanism over time. However, it is a useful method to compare the corrosion performance of materials in the acid test environments.

The Test 1 results show significant corrosion in all of the carbon steel test coupons (pipeline corrosion coupons) with a maximum corrosion rate estimated to be 28.8 mm/yr for the Low Carbon Steel A-36 in the bottom part of the pipe. All of the observed corrosion rates were well above the acceptance criteria of 0.1 mm/yr and therefore without treatment, the well fluid is unusable. High alloy material 22Cr-5Ni showed very low corrosion rate.

Weight loss of Linear Polarisation Resistance (LPR) electrodes was also measured and the results are summarised in Table 6. Weight loss measurement of the LPR electrodes showed that the corrosion rate for carbon steel in acid fluid (Test 1) was between 2.5 to 3.4 mm/yr. This value was less than the pipeline coupon results reported by Villa et al, 2000 primarily because of the lower flow encountered by monitors in different parts of the test chambers.

Table 5: Measured corrosion rate of the test coupons in the pipeline (PNOC-EDC and TNIRI results) for Test 1 over 360 minutes exposure period. 1 = Top, 2 = Side, 3 = Bottom of pipe.

Data from	Coupon Code	MatLoss µm	CorrRate mm/yr
PNOC-EDC test coupons	**L-80 casing**		
	L-1	4.007	5.854
	L-2	3.376	4.932
	L-3	4.151	6.064
	K-55 casing		
	K-1	3.960	5.786
	K-2	5.120	7.480
	K-3	3.402	4.970
	Wellhead Material		
	W-1	18.806	27.475
	W-2	6.659	9.728
	W-3	6.472	9.456
	Low Carbon Steel A-36		
	C-1	2.865	4.185
	C-2	4.166	6.086
	C-3	19.735	28.832
Data from	**Coupon Code**	**MatLoss µm**	**CorrRate mm/yr**
TNIRI test coupons	**Carbon Steel A SS400**		
	GA-1	13.140	19.197
	GA-2	9.510	13.894
	GA-3	11.790	17.224
	Carbon Steel B SK4		
	GL-S1	10.841	15.839
	GL-S2	8.997	13.144
	GL-S3	11.602	16.951
	API Standard N80		
	N8-35	13.696	20.009
	N8-36	8.739	12.767
	22Cr-5Ni		
	D5-13	0.006	0.009
	D5-14	wt gain	wt gain

Note: 360 minutes exposure period

Very low corrosion rates were observed on the high alloy materials Incoloy 825, Sandvik 2205 and Sandvik 2507 evaluated by LPR in Test 1 environment, with the two Sandvik alloys giving the best performance.

In Test 2, a much higher mass loss corrosion rate of carbon steel in brine fluid was observed by on-line monitors, which was due to the more aggressive brine fluid (Figure 5). The corrosion rates in the positions F1 and F2 determined by weight loss were lower due to difficulties in achieving reasonable flow through the discharge pipes. The mass loss corrosion rates observed in Test 3 were lower than those in Test 2 but of a similar magnitude to Test 1.

LPR On-Line Corrosion Rates

The Linear Polarisation Resistance corrosion monitoring method is based on electrochemical theories of corrosion, where the potential is moved away from the free corrosion potential by application of polarising current Δi to achieve a change in potential $\Delta\Phi$ of 10 mV (Lichti and Wilson, 1984).

$$R_p = \frac{\Delta i}{\Delta \phi}, \tag{3}$$

where R_p = Polarisation resistance (Ω), Δi = change in current (Amperes) and $\Delta\Phi$ = change in potential (V).

The corrosion current is proportional to a constant B divided by the polarisation resistance:

$$I_{corr} = \frac{B}{R_p}, \tag{4}$$

where I_{corr} = Corrosion current (Amperes), R_p = Polarisation resistance (Ω) and B = constant (V).

And the corrosion rate can be calculated using Faraday's Law as follow:

$$CR = \frac{I_{corr} M}{zF\rho A}, \tag{5}$$

where CR = Corrosion rate (mm/s), I_{corr} = Corrosion current (Amperes), M = Molar mass of material (g/mol), z = No of valence electrons, F = Faradays constant (96,500 A sec/mol), ρ = Density of material (mg/mm^3) and A = Surface area (mm^2).

The LPR instrument used has a pre-programmed "B" value of 35mV and an electrode area of 900mm^2 (Lichti and Wilson, 1984). Hence, correction was made to adjust the B value and the area of the working electrode for the test environments. The solution resistance was assumed to be low in the chloride rich water. The "B" value was measured by performing a step change in both anodic and cathodic polarisation on the electrode in test environments (-40 to +40 mV) and using the graphical curve fitting method of Mansfeld (Mansfeld, 1976). A "B" value of 15mV was calculated for carbon steel in acid fluid. This was consistent with data found in literature for acid fluids (Treseder et al, 1991). The corrosion rates obtained from the on-line results were then adjusted using the equation below:

$$\begin{aligned} CR_{corrected} &= CR_{measured} \times \frac{B_{actual}}{B_{assumed}} \times \frac{ElectrodeArea_{new}}{ElectrodeArea_{actual}} \\ &= CR_{measured} \times \frac{0.015}{0.035} \times \frac{900mm^2}{ElectrodeArea_{actual}} \end{aligned} \tag{6}$$

There were discrepancies in results obtained from the weight loss on LPR electrodes compared to the LPR instantaneous results (Table 6). LPR monitoring provided indicative corrosion rates, however the results obtained when corrected for the "B" constant were almost always lower than the mass loss corrosion rate from removable electrodes. In the brine environment (bottom of vessel), the LPR result showed a significant reduction in the corrosion rate of carbon steel when exposed to chemically treated geothermal fluid (Test 3). The corrosion rate was reduced from 0.43 mm/yr in acid fluid environment to 0.09 mm/yr in the treated fluid environment. Insufficient treatment (Test 2) resulted in a much higher LPR corrosion rate at this location.

The results for carbon steel in the F1 (well) Cross were higher in Test 3 when the flow rate was kept reasonable high.

Potential Measurement and UT Testing

The open circuit potential of the exposed material was measured using the Silver/Silver Sulfide reference electrodes and the average potential for materials in different test environments are shown in Table 7. High alloy materials showed much higher corrosion potential compared to carbon steel materials.

The UT measurements (Table 8) showed a thinning rate of 1.05 mm/day on average when exposed to acidic fluid (Test 1). When additional NaOH was added, the thinning rate declined to 0.21 mm/day (Test 3).

Electrical Resistance Corrosometer™ Probes

Figure 8 illustrates the trend in corrosion as measured by the Corrosometer™ probes for the three test environments. The graphs allow the corrosion results to be compared with theoretical equations for linear, parabolic and logarithmic kinetics. In all three test environments, Corrosometer™ probes located in the brine environment (bottom of the pipe) gave the highest material loss readings. Test 2 corrosion was higher than Test 1 while Test 3 was lower than both Test 1 and Test 2.

Linearly increasing material loss was observed for carbon steel in Test 1 (acid fluid). The highest material loss was in the brine (bottom of pipe). The steam (static condition) material loss was about five times less than in the brine. The corrosion rate of the 316 stainless steel in steam (in the flow) was an order of a magnitude lower than carbon steel.

In Test 2, the acid level increased and there was insufficient NaOH injected but the slope of the plotted data suggests a mixed linear-parabolic kinetic in spite of the higher magnitude compared to Test 1. It can be argued that protective films were being formed; however these films were not able to provide complete protection to the underlying steel.

Similar to Test 1 (acid fluid), the Test 2 (insufficient pH adjustment) carbon steel probes exposed to brine had the highest material loss. The probe that was exposed to static steam environment had the lowest material loss while the third probe that was presumed to be exposed in the flow of steam had material loss between these two extremes.

In Test 3, the Corrosometer results suggest several different corrosion mechanisms over the short time while NaOH was being injected. Material loss of the bottom probe (in contact with the liquid brine) and the top probe (in contact with static steam) were initially unstable but then showed an approximately logarithmic rate with this being somewhat upset towards the end of the tests.

The carbon steel probe exposed in the flowing steam environment had a much lower initial material loss than in the other two environments but the rate of corrosion was linear and by the end of the test, the magnitude of the material loss was the same as for the other two. The results of this probe do suggest some formation of protective corrosion product or scale on the metal surface towards the end of the test.

Table 6: Summary of the material loss and corrosion rate results using the weight loss and LPR methods.

Test	Exposure Condition	Exposure Time minutes	Material	Location	Wt Loss Method ML µm	Wt Loss Method CR mm/yr	LPR Method (corrected) ML µm	LPR Method (corrected) CR mm/yr
Test 1	No NaOH	240	Carbon steel	E Bottom of vessel	1.142	2.503	0.541	0.432
				F1 (well) Cross	1.558	3.415	0.321	0.741
			Incoloy 825	F2 (well) Cross	0.055	0.120	0.003	0.006
			Sandvik 2205	G1 (well) Cross	0.025	0.055	0.011	0.018
			Sandvik 2507	G1 (well) Cross	0.033	0.073	0.019	0.012
Test 2	with insufficient NaOH	600	Carbon steel	E Bottom of vessel	16.767	14.698	4.333	3.506
				F1 (well) Cross*	1.237	1.084	0.222	0.214
			Incoloy 825	F2 (well) Cross*	0.022	0.020	0.002	0.001
			Sandvik 2205	G1 (well) Cross	0.104	0.000	0.072	0.064
			Sandvik 2507	G1 (well) Cross	no data	no data	0.032	0.029
Test 3	with sufficient NaOH	180	Carbon steel	E Bottom of vessel	1.463	4.276	0.145	0.093
				F1 (well) Cross	5.200	15.195	0.360	0.929
			Incoloy 825	F2 (well) Cross	0.039	0.113	0.010	0.016
		630	Sandvik 2205	mod G1 (well)	weight gain	-	0.015	0.093
			Sandvik 2507	mod G (well)	weight gain	-	0.014	0.011

Note: ML = material loss
CR = corrosion rate
* = low flow through the cross

Table 7: Oxidation potential results of materials in test environments measured using Ag/AgS reference electrodes.

Test	Probe No	Materials	Location	Avg Potential (SHE) mV
Test 1	BP 14	Carbon Steel	Bottom	-230.0
	BP 15	Carbon Steel	F1 (well)	-190.5
	BP 18	Incoloy 825	F2 (well)	93.8
	BP 19	Sandvik 2205/2507	G1 (well)	95.3
Test 2	BP 18	Carbon Steel	Bottom	-336.8
	BP 15	Carbon Steel	F1 inside flow	-325.0
	BP 14	Carbon Steel	F1 outside flow	-82.5
	BP 19	Incoloy 825	G1 (well)	119.4
	BP 19	Sandvik 2205/2507	G1 (well)	-34.0
Test 3	BP 18	Carbon Steel	Bottom	-221.6
	BP 15	Carbon Steel	F1 (well)	-145.3
	BP 14	Incoloy 825	G1 (well)	-23.1
	BP 19	Sandvik 2205/2507	F2 (well)	24.4

Table 8: UT measurement results at different test locations.

Test Location	Thinning Rate (mm/hr) Test 1 (no NaOH)	Thinning Rate (mm/hr) Test 3 (with NaOH)	Diff (T3-T1)
A	0.020	0.008	-0.012
B	0.038	0.014	-0.024
C	0.064	0.004	-0.060
D	0.014	0.010	-0.004
E	0.029	0.006	-0.023
F	0.114	0.007	-0.107
G	0.020	0.006	-0.014
H	0.019	0.013	-0.006
I	0.046	0.013	-0.033
J	0.047	0.008	-0.039

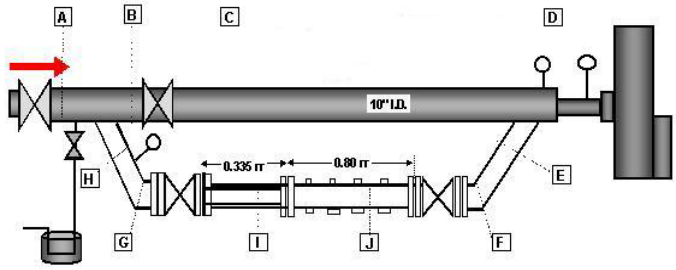

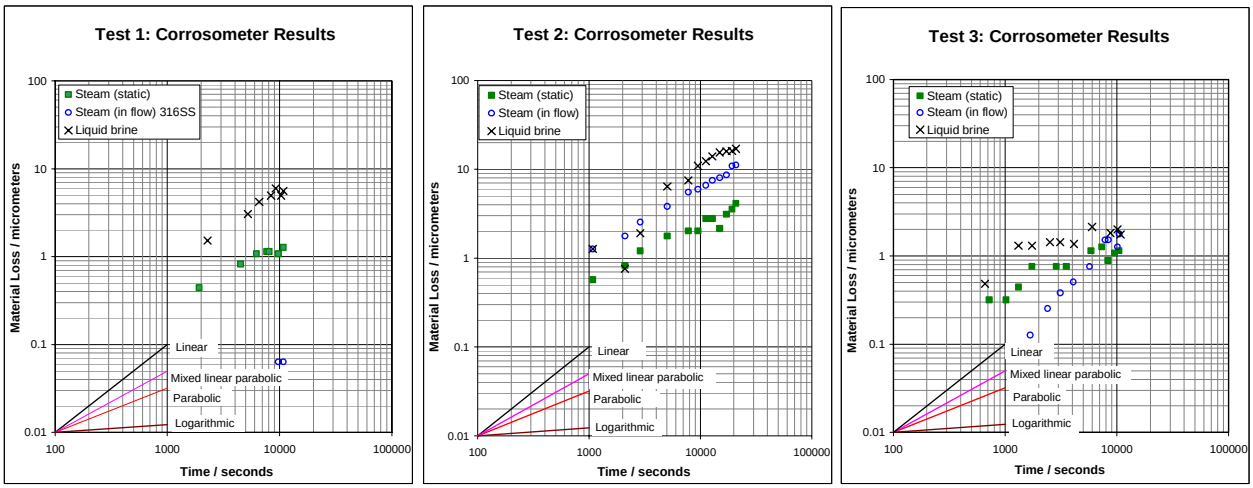

Figure 8: Logarithmic representation of material loss results from the Corrosometer™ readings (all probes are carbon steel unless noted).

Figure 9 provides a linear plot comparing carbon steel material loss in brine from Test 1 and Test 3 to demonstrate the effect of addition of sufficient NaOH to alter the solution chemistry. This result demonstrates that adjustment of the pH of the fluid can change the corrosion mechanism of carbon steel.

The decrease in corrosion rate of the carbon steel was argued to be due to the formation of protective corrosion product film as have been subsequently demonstrated in laboratory trials (Lichti, Klumpers and Sanada, 2002) however the analysis of the deposits formed as discussed below suggest a different interpretation.

4.2 Pitting Results

Corrosion pits were observed on all of the carbon steel electrodes as well as the Corrosometer probes. Pit densities and pit depths on the samples were measured according to ASTM Recommended Practice for Examination and Evaluation of Pitting Corrosion (G46-76). The results are summarised in Table 9. The average of the 5 deepest pits observed and the maximum of these 5 are reported.

Under the acid conditions of Test 1 and 2, there were a small number of deep pits on carbon steel electrodes (Table 9) with a maximum pit depth of 68 µm in Test 2. Addition of NaOH at a level sufficient to reduce the material loss did not preclude pitting corrosion, however, the formation and propagation of these pits changed so there was a higher density of shallower pits observed on carbon steel exposed in Test 3. Insufficient pH adjustment (Test 2) induced localised anodic sites and promoted the propagation of pits. The high alloy materials exposed in brines showed no sign of pitting corrosion.

4.3 Corrosion Products Characterisation

The LPR probes used 3 electrodes. Two of these were cleaned while the third was kept for analysis of the surface films. Deposits on Corrosometer probes as well as the electrodes and probes that were to be cleaned were collected by scraping and on two-sided tape.

Non-uniform corrosion scales were observed on the carbon steel electrodes exposed to acidic environment (Test 1). SEM EDX analysis showed that the surface corrosion product generally contained high levels of iron (Fe) and oxygen (O). Heavy metals such as lead (Pb) and arsenic (As) were also observed with minor amounts of sodium (Na), silicon (Si) and manganese (Mn). Arsenic has long been used for corrosion inhibition and silica is known to form as a barrier film on carbon steel and limit corrosion in some geothermal brines that are saturated with silica. In some areas, a thin and dense layer of corrosion product was observed on the surface of carbon steel that contained a high level of silicon (Si) which contributed to the stability of the corrosion product films even in this acidic environment.

The results from prepared cross sections were consistent with the surface analysis. A summary of the EDX analysis of the cross section scales that formed in the corrosion tests is shown in Table 10. The results show non-uniform intermittent corrosion products which contained mainly iron and oxygen (Figure 10a). In some areas, bright spots were seen in the SEM images which contained higher sulphur and heavy metals lead and arsenic (Figure 10a). However the corrosion products were not protective and where corrosion products covered the surface, these were cracking away from the surface. It appeared that under acid well conditions, the dissolved iron ions (from the acid corrosion) tended to precipitate as iron oxides with local deposits of heavy metal sulfides.

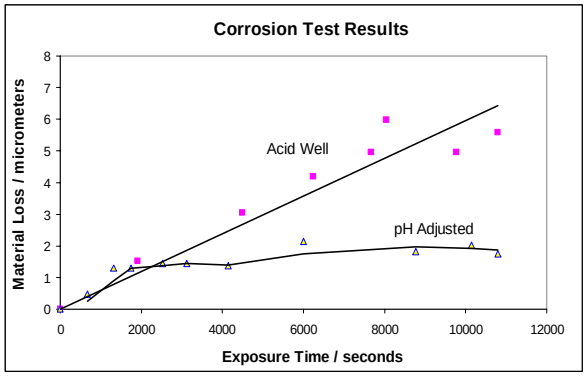

Figure 9: Corrosion test result comparison of the acid well result (Test 1) and the pH adjusted result with sufficient NaOH added into the well (Test 3).

Table 9: Pitting data of carbon steel LPR electrodes and Corrosometer™ probes exposed in MG-9D geothermal fluid.

Exposure Condition	Location	Electrode No. Code	Pit Depth				Pit Density ASTM G36
			Avg (µm)	Max (µm)	Avg (µm)	Max (µm)	
			Individual Electrodes		Combined Electrodes		
Test 1	E-Bottom	1-50	33.8	42	34.4	42	larger pits A2/A3 small pits initiated A5
		1-51	15.6	30			
	F1-Cross	1-54	25.4	35	31.6	35	A1/A2 small pits A5
		1-55	21.6	32			
Test 2	E-Bottom	1-57	25.8	42	45.8	68	larger pits A2 small pits A5
		1-58	37.4	68			
	F1-Cross	1-60	7.6	14	38.4	67	A2/A3
		1-61	37.8	67			
Test 3	E-Bottom	1-66	10.4	12	20.2	29	A5 all surface
		1-68	19.6	29			
	F1-Cross	1-70	14.8	17	21.8	24	A5
		1-74	21.8	24			

Corrosometer			Pitting (µm)		Pit Density
Test No.	Exposure	No.	Mean	Max	
Test 1	Liquid Brine	Aug 81 #4	40	72	A3
	Flowing Steam	Oct 86 #1	39	62	A3/A4
	Static Steam	310 #10	31	39	A2
Test 2	Liquid Brine	Oct 86 #2	54	68	A3/A4
	Flowing Steam	March82#6	88	119	A4/A5
	Static Steam	Oct 86 #3	36	76	A3/A4
Test 3	Liquid Brine	Oct 86 #4	51	85	A4/A5
	Flowing Steam	Aug 81 #1	30	42	A2

Note: Test 1 - 240 minutes Test 3 - 180 minutes
Test 2 - 600 minutes Pits with greatest depth were selected for measurement.

Table 10: SEM EDX elemental analysis data on cross sections of carbon steel test samples.

Test Environment	Electrode No.	Image	Location	Elements At%							
				O	Fe	S	As	Pb	Si	Zn	K
Test1 Bottom	1.53	12a	Bulk inner layer	61.6	37.2						
			Bulk outer layer	63.0	33.1	0.6	2.2	0.5			0.4
			Bright spots (specks)	Pb/As/S too small to analyse							
Test1 F1Cross	1.56		Dark grey bulk CP (similar to others)	67.1	32.3	0.3			0.4		
			Bright spots (specks) - heavy metals	55.7	39.3	2.1	2.1		0.8		
Test2 Bottom	1.59	12b	Bright top (porous) layer/areas	57.4	25.3	3.2	9.9	3.7	0.6		
			Bulk dark grey areas	64.5	35.2						
Test2 F1Cross	1.62		Thin dark CP general (no bright spots)	64.1	33.1	1.6			1.2		
Test3 Bottom	1.67	13	Bright layer in mid of the CP	18.0	21.6	29.4	8.5		0.7	21.5	
			Dark CP same as others	Fe/O							
Test3 F1Cross	1.69		Bright areas (very)	22.1	44.2	32.5			1.2		
			Lighter areas in the CP	S/Fe/O/Si							
Test3A Bottom	1.79		Darker layer in the marblelike layering	65.6	17.6		0.4		15.6		0.7
			Bright top (porous) layer/areas	higher in heavy metal (Pb, As etc)							
Test3A F1Cross	1.82		Dark areas	Fe/O							
			Bright line in mid of CP	S/Zn/As and trace of Pb							

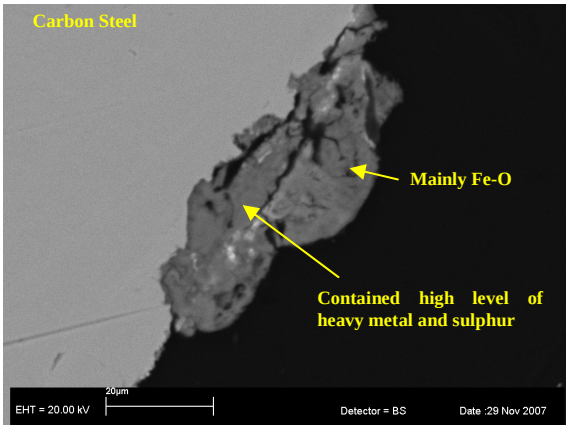

a. Cross section of sample 1-53 (Test 1) showing intermittent corrosion products.

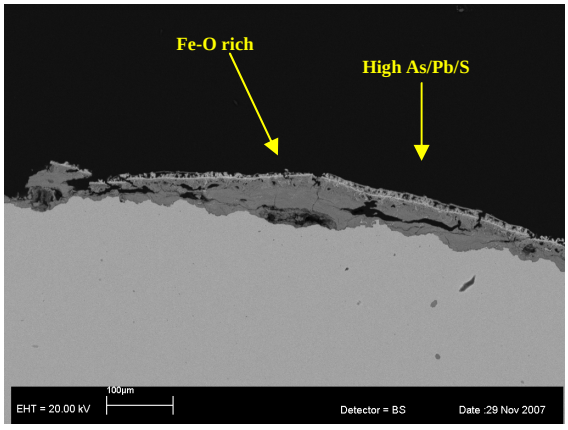

b. Cross section of sample 1-59 (Test 2) showing porous and fragile layer of sulfide corrosion product.

Figure 10: SEM images of cross section of carbon steel exposed under different test environments.

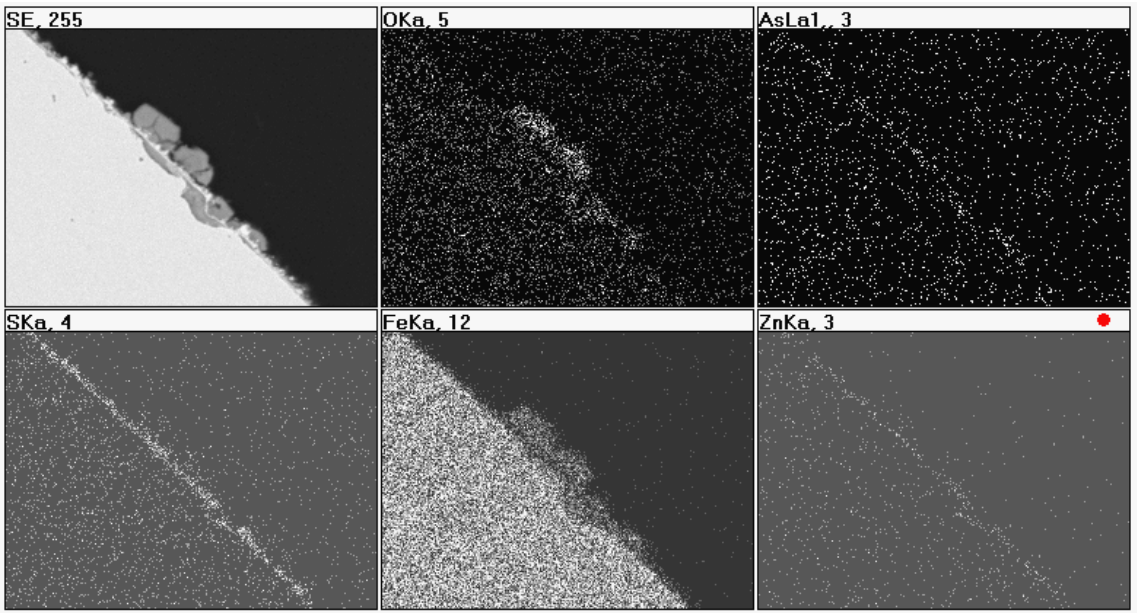

Figure 11: SEM elemental map of sample 1-67 under Test 3 environment showing a thin protective iron and sulphur rich layer containing low levels of arsenic and zinc.

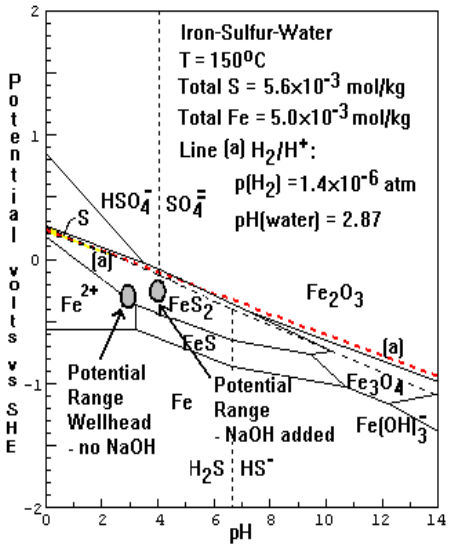

Figure 12: Potential-pH diagram for Mahanagdong Well MG-9D Wellbore chemistry.

XRD analysis showed that the corrosion products from the acid corrosion test were predominantly crystalline with the major compounds present being Magnetite (Fe_3O_4) and Hematite (Fe_2O_3) with a minor amount of Goethite (FeO(OH)).

Addition of NaOH in both Test 2 and Test 3 promoted the formation of iron sulfides on top of the iron oxide containing corrosion product. In Test 2 where insufficient NaOH was added into the solution, the sulfide layer observed on the sample was intermittent, very porous and weak (Figure 10b). It did not provide sufficient protection to the metal or the iron oxide corrosion product underneath to control corrosion and indeed the rate increased because of the more aggressive well fluids. Trace amounts of Halite (NaCl) were also found in the sample evaluated for Test 2.

The iron sulfide compounds were identified to be Pyrrhotite ($Fe_{(1-x)}S$) and Troilite (FeS) by XRD. The heavy metals arsenic and lead were also observed in the sulfide rich layers. When sufficient NaOH was added to the solution (Test 3) to give a lower corrosion rate, the iron sulfide layer generally covered the surface of the metal and appeared to be more adherent (Figure 11). This layer covered the underlying corrosion product and the steel, giving a reason for the reduced rate of corrosion, but the contribution of arsenic, lead and silica to the reduced level of corrosion was not determined from this work.

4.4 Thermodynamic Stability of Corrosion Products

The potential-pH diagram for the produced wellbore water (Fe-S-H_2O system) having total S concentration of $5.6x10^{-3}$ mol/kg and temperature of 150°C is reproduced in Figure 14 (Lichti and White, 1998). In the reducing environment (negligible oxygen) common to geothermal fluids, the corrosion potential should remain at or below the hydrogen evolution line (lower limit of the dotted line) in the potential-pH diagram.

Under equilibrium production conditions at pH range of 2.8 to 3.1, the MG-9D fluid gave a measured corrosion potential for carbon steel in the range of -0.19 to -0.30 V which is in the free corrosion region and the diagram is consistent with acid corrosion (Figure 12).

Sufficient addition of NaOH inhibitor to move the brine solution pH to 4.0 gave a corrosion potential for carbon steel in the range of -0.15 to -0.25 V. At this pH and potential, stable formation of iron sulfide compounds would be predicted. The diagram represents thermodynamic equilibrium and the short term experiments do demonstrate progression to protective iron sulfide film formation which lowers the rate of corrosion. However, the contribution from arsenic, zinc and lead containing compounds as well as silicon remain to be fully defined.

5. CONCLUSIONS

The following may be concluded from the acid well corrosion tests of the Mahanagdong Well MG-9D:

- Under acid fluid environment, the corrosion rate of carbon steel was estimated to be as high as 28 mm/yr, which was well above the acceptance level of 0.1 mm/yr. The corrosion was non uniform with intermittent corrosion products remaining on the surface mainly containing iron oxides.
- The injection of NaOH for chemical treatment of the well must be at sufficient quantities to achieve the desired pH to obtain effective corrosion control. Insufficient NaOH resulted in weak and non-protective film formation and the initiation of local pits that readily propagated.
- Sufficient NaOH injection was successful in raising the pH of the solution from pH 2.8 to 4.0. UT measured thinning rate dropped from 1.05 mm/day to 0.21 mm/day. Consistent results were found with the LPR on-line corrosion monitoring and Corrosometer™ monitoring.
- Not all corrosion monitors indicated low corrosion rates under pH adjusted condition and some impacts of velocity were noted.
- Addition of NaOH promoted the formation of protective iron sulfides films and helped to stabilised the underlying iron oxides corrosion product that reduced the rate of corrosion.
- High levels of heavy metals arsenic and lead as well as zinc and silicon were observed within the corrosion products and these may have contributed to the stability of corrosion products which reduced the corrosion rates or they may have acted as inhibitors to acid corrosion at the raised pH levels.
- The corrosion potential of the acid fluid was in the region of free corrosion with a minimum of passive film formation. The addition of NaOH successfully raised the pH of the solution to 4.0 and at this potential iron sulfide stability was observed as was predicted.
- High alloy materials such as Incoloy 825, Sandvik 2205 and Sandvik 2507 had very low corrosion rate and show potential for non pressure components in acid well environments of pH 3 to 4.

6. ACKNOWLEDGEMENTS

The work described was undertaken under joint funding from PNOC-Energy Development Corporation, Philippine Geothermal Inc., the New Zealand Foundation for Research Science and Technology (NZ FRST) and from AIST, MITI, Japan. This paper was prepared with financial support of Institute of Geological and Nuclear Sciences under NZ FRST subcontract. The authors express their thanks to Contact Energy New Zealand for engineering support and to PGI Unocal (now PGI Chevron) for their on site assistance.

REFERENCES

Braithwaite, W.R. and Lichti, K.A. (1980). Surface Corrosion of Metals in Geothermal Fluids at Broadlands, New Zealand. Geothermal Scaling and Corrosion, ASTM STP 717, pg 81-112.

Crowe, D.C and Tromans, D. (1986). The Silver Sulfide Reference Electrode for Use in Alkaline Sulfide Solutions, Corrosion – NACE Vol. 42(7), pg 409-415.

Kurata, Y., Sanada, N., Nanjo, H., Ikeuchi, J. and Lichti, K.A. (1995). Material damage in a volcanic environment. Proceedings of the World Geothermal Congress, 4.

Lichti, K.A., Klumpers, A. and Sanada, N. (2002). Utilisation of Acidic Geothermal Well Fluids: Progress to 2002. Proceedings, 24th NZ Geothermal Workshop.

Lichti, K.A. and Sanada, N. (1997). Materials Issues for Utilization of Deep Geothermal System for Utilisation of Deep Geothermal System. Proceedings, 19th NZ Geothermal Workshop.

Lichti, K.A and White, S.P. (1998). Modelling of Acid Fluid Wellbore Chemistry and Implications for Utilisation. Proceedings of the 20th NZ Geothermal Workshop.

Lichti, K.A., White, S.P. and Sanada, N. (1998). Corrosion in deep and acidic geothermal wells. Proceedings of the 19th Annual PNOC-EDC Geothermal Conference.

Lichti and Wilson (1984) The Determination of Metal Corrosion Rates in Geothermal Condensate Using Electrochemical Techniques, Proceedings of NZ Geothermal Workshop.

Mansfeld, F. (1976) The Polarisation Resistance Technique for Measuring Corrosion Rates in Fontana, M.G. and Staehle, R.W.eds., Advances in Corrosion Science and Technology, Plenum Vol. 6, pg 163-262.

Moya, P, Nietzen, F, Eddy Sánchez, E (2005) Development of the Neutralization System for Production Wells at the Miravalles, Geothermal Field, World Geothermal Congress Proceedings World Geothermal Congress,Antalya, Turkey, 24-29 April

Parrilla, E.V. and A.T.N. Salazar (1996). Geochemical Evaluation of Corrosion Tests in Well MG-21D, LGPP. PNOC-EDC Internal Report.

Salonga, N.D., Parrilla, E.V. and Martinez, M.M. (1997). Acid Fluids in Tongonan Mahanagdong and Alto Peak Geothermal Fields, Lyte, Philippines. Proceedings, 18th PNOC-EDC Geothermal Conference.

Sanada, N, Kurata1, Y, Nanjo, H, Kimi, H, Ikeuchi1, J, and Lichti, K A. (2000) IEA Deep Geothermal Resources Subtask C: Materials, Progress with a Database for Materials Performance in Deep and Acidic Geothermal Wells, World Geothermal Congress, Kyushu - Tohoku, Japan, May 28 - June 10, pp 2411-2416.

Sánchez, E, Guido, H., and Vallejos, O. (2000) Commercial Production of Acid Wells at The Miravalles Geothermal Field, Costa Rica, World Geothermal Congress, Japan.

Treseder, R.S. (eds.), Baboian, R. and Munger, C.G (co-eds). NACE Corrosion Engineer's Reference Book (Second Edition). Houston: Texas, 1991, pg 65-66.

Villa, R.R. (1999). 1999 Annual Report, Mahanagdong A and B Process Chemistry. PNOC-EDC internal report.

Villa, R.R. et al. (2000). A Demonstration of the Feasibility of Acid Well Utilization: The Philippines' Well MG-9D Experience. Proceedings of the 21st Annual PNOC-EDC Geothermal Conference.